Microwave Review
July 2025, Vol. 31, No. 1, pp. 63-67
DOI: 10.18485/mtts_mr.2025.31.1.11

Broadband Low Loss Compact Size 2nd-Order Planar Bandpass Filter for Ku-Band Applications

Rashmita Mishra[1], Ajit Kumar Patro[2], Kailash Chandra Rout[3]

Abstract – **This paper presents the design and analysis of a low-loss; compact-size broadband second-order band pass filter (SOBPF) utilizing a simple microstrip line concept for Ku-band and satellite communication applications. For the Ku-band frequency range, the design method is used as an easy way to generate two transmission poles and the SOBPF. The input impedance of the conventional T-shaped microstrip feed is implemented and determined at 50 ohms in the early stages. Then, two rectangular closed strip lines are implemented symmetrically and placed at the center on the top plane of the radiating part. These strips play a significant role in creating the coupling between them. Hence, these strips generate two poles and develop an SOBPF. In addition, an open circular-shaped stub is also used in a cuboid shape in order to improve impedance matching. The experiment is used to verify the results of the analysis and simulation of the design structure. The simulated and measured -10 dB reflection coefficient (|S_{11}|<-10 dB) of absolute impedance bandwidth (AIBW) are 2.9 and 3.2 GHz, respectively. The minimum and maximum simulated insertion loss (IL) of 0.12 and 1.89 dB are obtained. Meanwhile, the measured minimum and maximum IL of 0.24 and 1.31 dB are achieved. The simulation results are evaluated and compared with the filter characteristics testing data.**

Keywords: **Broadband; compact size; Insertion loss; Impedance matching; Second order, total loss.**

I. Introduction

The proliferation of advanced communication networks has led to a surge in the need for band-pass filtering systems capable of efficiently processing large volumes of data or information. Bandpass filters (BPFs) play a crucial role in components of RF and microwave systems [1], as they are necessary to meet various standards. Several works have proposed different approaches for synthesizing and building bandpass filters (BPFs).

There have been developments in the use of BPFs, which come with different levels of sophistication. Furthermore, space applications commonly utilize large, unwieldy filters with specialized band-pass sections. The reduction of size and mass is of utmost importance in such scenarios. This work explores filters characterized by high performance, low weight, and small size.

Article history: Received September 13, 2024; Accepted October 28, 2024

[1]Rashmita Mishra, is with the Ph.D research scholar in the Dept. of Electronic and communication Engineering, GIET University, Gunupur, Odisha, India-765022, E-mail: rasmita.mishra@giet.edu

[2]Ajit Kumar Patro and [3]Kailash Chandra Raut are with the faculty in the Dept. of Electronic and communication Engineering, GIET University, Gunupur, Odisha, India-765022,
E-mail: [2]ajitpatro@giet.edu; [3]kailash.rout@gmail.com

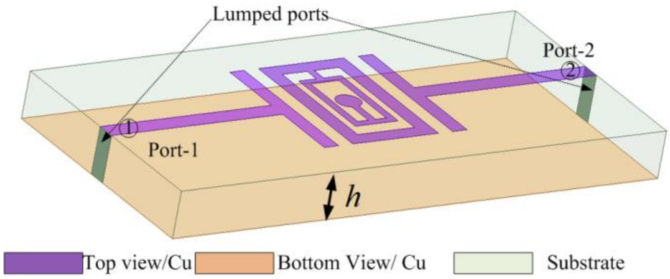

Fig. 1. 3D view of the proposed bandpass filter.

This work proposes tiny broadband waveguide filters for satellite applications operating in the C-/Ku-band frequency range. The essential requirements that must be fulfilled concurrently in both C- and [12] a decrease in mass and volume. TM resonators are a practical choice in terms of compactness and bandpass. They allow for a significant reduction in filter length, up to 75%, compared to standard filters that use TE mode cavities [2]–[6]. Additionally, TM resonators maintain high Q-factor values (>4000). While these resonators can meet the criteria for mass, volume, and loss, they cannot meet the extensive stop-band requirements of the project. In order to expand the stop band, it has been proposed in [7] to use multi-aperture irises instead of single-aperture irises. Regrettably, this project still requires further refining. Narrow BPF with low profile employing FSS structure [8], vertically integrated substrate-integrated suspended line BPF [9], SIW-based BPF [10], multilayer-dual-band BPF [11], and ultra-compact SIW-BPF [12] are among the recent efforts that have been reported [8]– [12]. Recently, a few works have been reported [13]–[19], such as microstrip BPF using spoof surface plasmon polaritons (SSPP) [13], a dual-band BPF (DBBPF) using dual-band negative group delay equalizers [14], high-temperature super-conducting 4th-order narrowband BPF using a spiral-CRLH resonator [15], a low-loss organic substrate-based BPF [16], SIW-based compact narrow-band BPF using SSPPs [17], a DBBPF-based on suspended coplanar waveguide-microstrip [18], ultra-wideband compact-BPF [19], SIW-based BPF using power divider [20], and high selectivity BPF[21].

This study introduces a new low-loss, compact size, and broadband second-order band pass filter (SOBPF) using a broadband resonator class that rejects the spurious band and achieves an acceptable transmission coefficient for Ku-band applications. The resonators are built on 3.2 GHz bandpass filters with T-shape-coupling feeders. The modeling and observed data show that these designs have produced more than −24 dB suppression in the first spurious pass band.

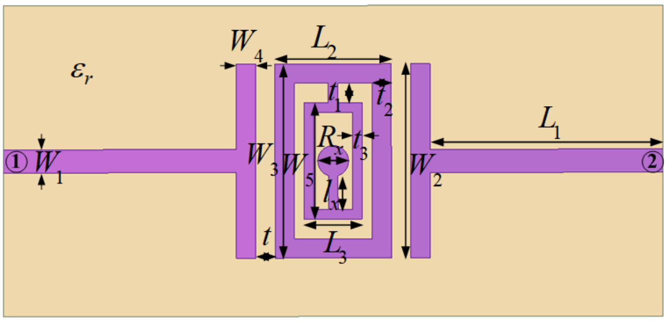

Fig. 2. Geometric of proposed SO-BPF (front view)

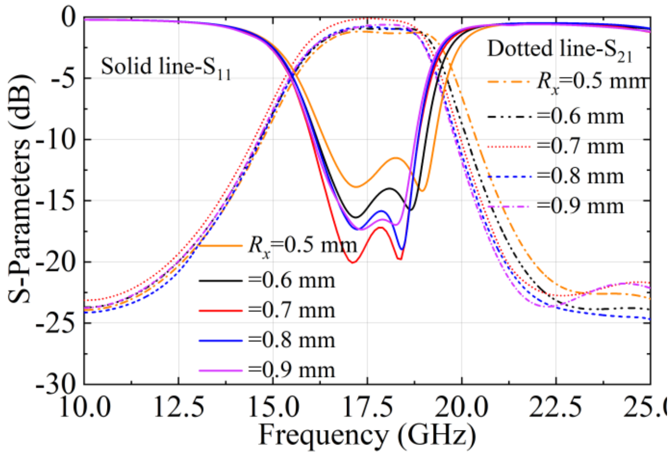

Fig. 3. Reflection coefficient effect on R_x

The study work applies to IEEE 802.11ac higher standards. Several research studies [6]-[12] have examined various band planar filters for various applications utilizing different hairpin architectures. However, the setups still take up a significant amount of circuit space, so they are essentially unsuitable for systems where downsizing is crucial. It has proven to be a crucial problem when creating microwave filters. The proposed SOBPF concepts are suitable for broadband broadcasting communication satellites, according to the results of the practical environmental testing (thermal, sine, and random vibration) conducted on both filters. This work provides a comparison table at the end, which compares similar types of reported works.

II. Ku-Bandpass Filter Design and Parametric Analysis

Figures. 1 and 2 depict the three-dimensional (3D) and top views of the proposed second-order BPF (SOBPF), respectively. The total ground plane makes up the bottom plane. For the design and analysis, the schematic design arrangement of a small microstrip hairpin slots second-order bandpass filter is shown in Fig. 2. It was made on a Rogers 5880 (TM) substrate (17 mm × 8 mm × 1.524 mm) with a thickness of 1.524 mm, a loss tangent of 0.0004, and a relative dielectric constant of 2.2. In the first stage, two symmetric T-shaped feeder lines next to each other in a window configuration act as coupling resonators, changing the passband to the right one while keeping the 50 Ohms impedance matching with the input/output devices.

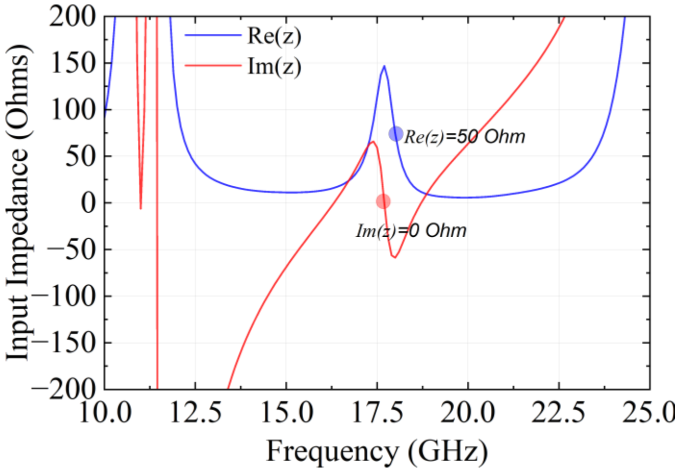

Fig. 4. Simulated input impedance vs. frequency response (blue: real and red: imaginary)

The designed SOBPF propagates TM mode cavity resonators using microstrip planar technology. The window hairpin slots resonator, and the symmetric T-shaped feeder line resonators were put together in this study to get a selective resonance frequency with good spurious suppression in the stop-band response. The hairpin-slots window configuration's broadband resonant frequency and usable bandwidth can be readily adjusted in the analysis by varying the overall width or the overall length of the designed SOBPF. As a result, insertion and return loss variations are encountered. The electric and magnetic couplings can be obtained if the open sides of two linked resonators are placed as close together as possible, as shown in Fig. 1.

In the second step, we implement two symmetrical rectangular closed strip lines and place them at the center on the top plane of the radiating part. These strips play a significant role in creating the coupling between them. Hence, these strips generate two poles and form an SOBPF. The gap between two strips also helps increase or decrease the coupling effect. Therefore, we use parametric analysis to fix the gap between the two strips. In addition, an open circular-shaped stub is also used in cuboid shape in order to improve impedance matching. The radius of the open circular stub plays a crucial role in improving impedance matching. In light of this, a parametric analysis is used to fix the radius of the open circular stub R_{xx}, as shown in Fig. 3. The R_{xx} varies from 0.5 to 0.9 mm with a step size of 0.1 mm. We fix the R_{xx}=0.7 mm for better impedance matching. Plotted in Fig. 4, the real part of the input impedance at the pass band frequency range is around 50 Ω when the diameter R_{xx} is 0.7 mm, while the imaginary part is approximately zero. Finally, the optimized dimensions of the proposed work are listed below: W_1=0.6 mm, L_1=6mm, L_2=3.5 mm, W_2=5 mm, W_3=5 mm, W_4=0.5 mm, L_3=1.5 mm, W_3=3 mm, t =0.5 mm, t_1 =0.5 mm, t_2 =0.5 mm, t_2 =0.25 mm, R_x=0.7 mm L_x=0.85 mm. Furthermore, the surface current and electric field distributions of the proposed antenna is plotted at the center frequency, as shown in Fig. 5 (a) and (b), respectively. It is confirmed that the structure propagates the *TM* mode. All the simulations were carried out using Ansys HFSS 2020R2 electromagnetic software.

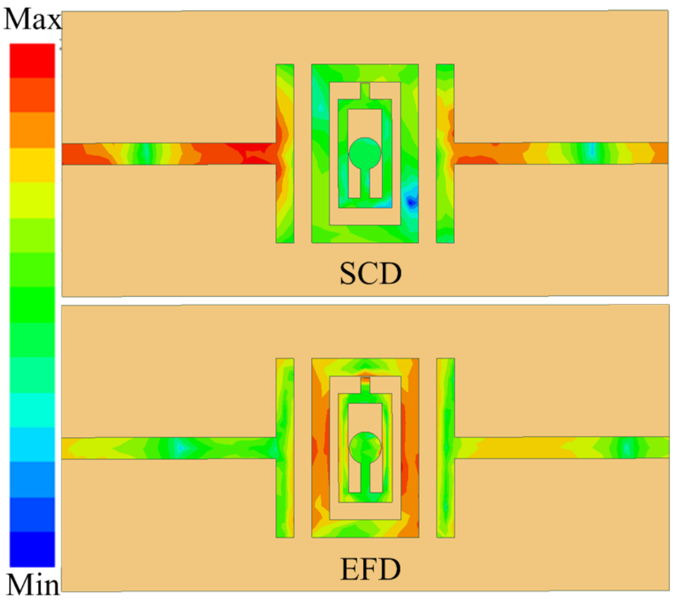

Fig. 5. Electric field distribution (top) at 6 GHz and 16.25 GHz (center frequency)

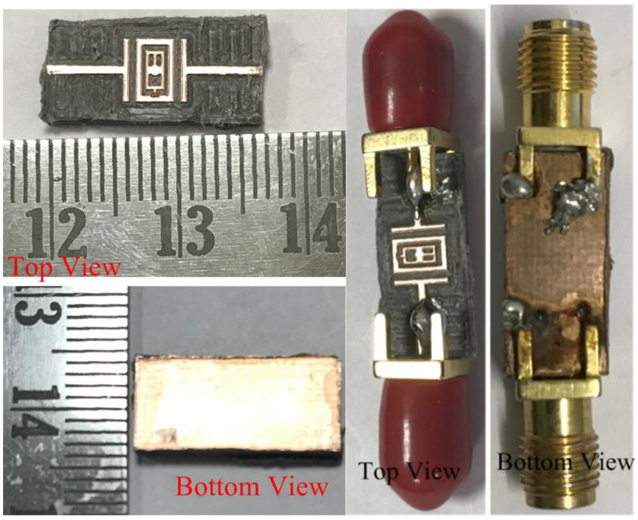

(a) (b)

Fig. 6. The fabricated prototype of the proposed SOBPF: (a) without connector (b) with connector

III. Simulation and Experimental Results

The top and bottom views of the fabrication prototype of the proposed antenna are depicted in Fig. 6. The antenna is measured in the S_{11} and S_{21} with a vector network analyzer, the Agilent N5247A (10 MHz–67 GHz). This design obtains and achieves the maximum simulated and measured return losses of 22 and 20 dB. The simulated 10 dB ($|S_{11}|$<-10 dB) return loss absolute impedance bandwidth (AIBW) and insertion loss (IL) of 0.12/1.89 and 0.24/1.31 dB are achieved, respectively. The recorded minimum and maximum insertion loss are 0.24 and 1.31 dB, respectively. This result includes two 6.15 mm long 50-ohm feeding lines for the probe measurement [20]-[21]. The minimum and highest insertion losses are approximately 0.01 and 0.05 dB/mm throughout the

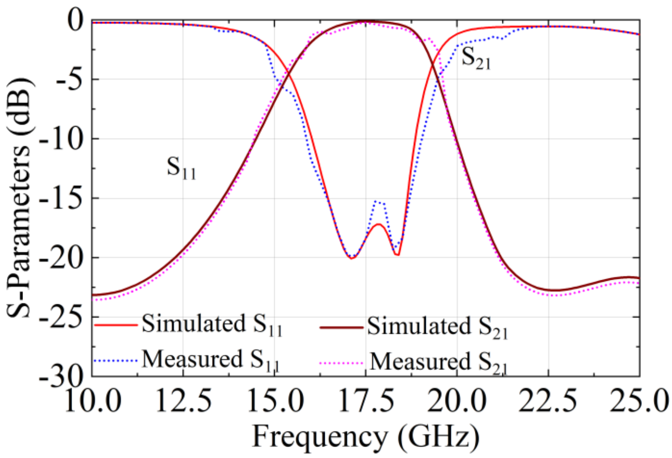

Fig. 7. Simulated and measured S-parameters (magnitude of $|S_{11}|$ and $|S_{21}|$) of SOBFP

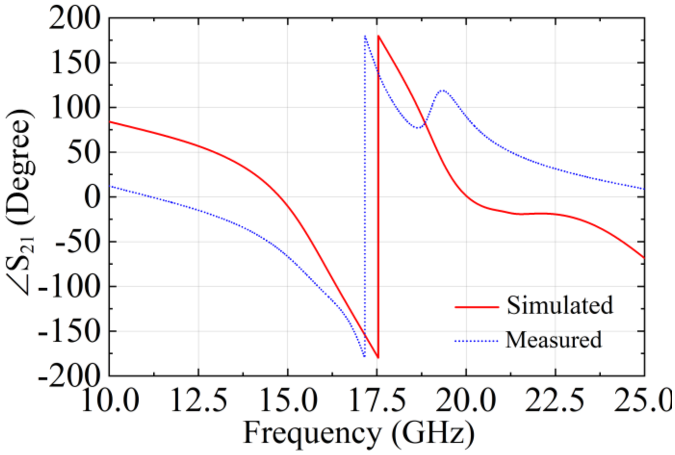

Fig. 8. Simulated and measured phase of S_{21} (degree) of the SOBPF

bandwidth. In addition, the simulated and measured phase is matched, and it varies from -176^0 to 179^0. The experimental validity is verified by utilizing the modelling results of this developed BPF structure, the phase of S_{21}, as shown in Fig. 8. This graphic demonstrates how exactly the S_{21} simulated phase corresponds. The group delay vs frequency plot is plotted, as shown in Fig. 9. Furthermore, the pass band achieves the simulated and measured minimal group delays of 0.14 and 0.10 ps, as illustrated in Fig. 9. Conversely, the measured and simulated group delays have maximum values of 0.24 and 0.33 ps, respectively. Consequently, the flat group delay and excellent linearity of this proposed BPF have enhanced the filter qualities. The total loss is also calculated in the proposed work.

The overall loss combines leakage, metallic or copper, and dielectric loss. In light of this, we investigated the contributions of these sources of transition losses, consecutively adding one source to another. The overall loss (or total loss $=1-|S_{11}|^2-|S_{21}|^2$) [22]-[25] are computed using three steps as follows:

1. Assume that the top cladding conductor (TCC) and bottom cladding conductor (BCC) are ideal conductors. Assume the perfect dielectric without any losses. Simulate and calculate the total loss. This will give the leakage loss.

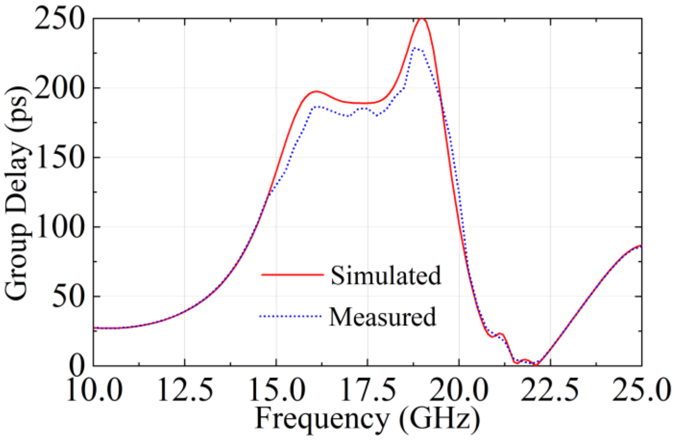

Fig. 9. Simulated and measured group delay (ps) of the SOBPF

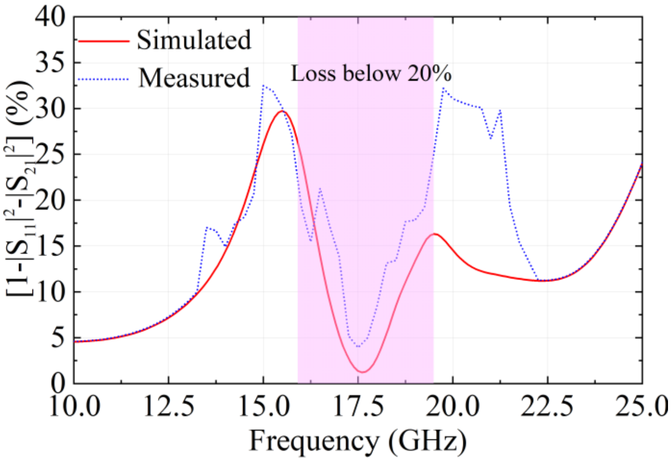

Fig. 10. Simulated and measured total loss (in %) of the SOBPF

2. Assume the finite conductivity (Cu) with dissipation factor (tanδ) and simulate and calculate the total loss again. This will cause leakage loss plus copper loss.

3. Assume the finite conductivity (Cu) with dissipation factor (tanδ). Assume the dielectric with losses (tanδ). Simulate and calculate the total loss.

This sequence of simulations will allow us to evaluate the contribution of each source to the total loss. From the above statements, the total loss depends on both $|S_{11}|$ and $|S_{21}|$. So, the total loss is $(1-|S_{11}|^2-|S_{21}|^2)$ (in %), as shown in Fig. 10.

TABLE 1
COMPARISON OF THE PROPOSED WORK WITH THE STATE-OF-THE-ART

Ref.	**Size (λ_0^2)**	***h* (mm)**	**f_0 (GHz)**	***FIBW* (%)**	***IL* (dB)**
[13]	0.19	0.508	3.97	36.77	2-2.5
[14]	1.18	0.508	2	50	1.5
[15]	0.0978	0.5	0.218	0.5	0.3
[16]	0.0272	0.3	6.54	20	2.6
[17]	0.266	0.254	30	3	>1.5
[18]	0.049	0.787	3.4	17.6	0.39-1.3
[19]	0.077	0.813	3	40	2-9
This work	**0.462**	**1.524**	**17.5**	**18.28**	**0.24-1.31**

IL: Insertion loss, *FIBW*: Fractional impedance bandwidth, f_0: Resonant frequency

The total loss has carefully verified both simulation and experimental results. As a result, the total loss simulated below 22% is achieved in the entire frequency range. In contrast, the total loss measured below 20 % is achieved at 15.9–19.1 GHz. The simulated and measured total losses are slightly high due to the fabrication tolerance.

Table 1 presents a comparison of the proposed SOBPF performance with earlier work in order to better illustrate its advantages. In comparison in terms of compact size in [13], [14], and [17], FIBW Refs. [15], [17], and [18], and low IL Refs. [13], [14], and [16]-[19]. In contrast, the proposed work has a slightly larger issue than in Refs. [15], [16], [18], and [19], has a lower FIBW than [13], [14], [16], and [19], and has a slightly higher IL than [15]. The total loss is calculated and included in Table 1. It is confirmed that the total loss is below 20% of the proposed work. Hence, the presented work has a more significant advantage in size, low overall loss, and provides broadband performance in the higher frequency range. In addition, our BPF provides more pronounced out-of-band suppression effects in this work. Due to these combined benefits, our suggested design is a strong contender for several real-world microwave communication applications.

IV. CONCLUSION

This paper designs simulates, fabricates, and tests a compact size, low loss, and broadband second-order bandpass filter for Ku-band applications. This structure uses the symmetric T-shaped-feeder-coupled line resonator-based microstrip line and the outcomes of the experiment validation with the simulation match those that were anticipated. With feeder lines excluded, the geometrical dimensions of the primary window structure are $\approx 0.99\lambda_0 \times 0.46\lambda_0$ for SOBPF. The symmetric T-shaped feed line resonator window resonator design is presented as an alternative to the filter structure's miniaturization. Therefore, this resonator can minimize a notably small filter size. The proposed SOBPF can be used for various wireless services, radar, and satellite communication applications

ACKNOWLEDGEMENT

Rashmita Mishra would now take this opportunity to express gratitude to BPPIMT'S authorities for providing the scope to pursue my Ph.D. work at GIET University and the required support. We also thank all reviewer for their comments on the potential of our manuscript.

REFERENCES

[1] M. Uhm, K. Ahn, I. Yom, and J. Kim, "A Triple-Passband Waveguide Filter with Dual-Mode Resonators for Ka Band Satellite Applications", *Proc. 24th AIAA Int. Commun. Satell. Syst.* Conf., June 2006, p. 5450, DOI: 10.2514/6.2006-5450

[2] S. Bastioli, C. Tomassoni and R. Sorrentino, "A New Class of Waveguide Dual-Mode Filters Using TM and Nonresonating Modes", *IEEE Transactions on Microwave Theory and Techniques*, vol. 58, no. 12, pp. 3909-3917, Dec. 2010, DOI: 10.1109/TMTT.2010.2086068

[3] U. Rosenberg, S. Amari and J. Bornemann, "Inline TM/sub 110/-mode filters with High-Design Flexibility by Utilizing Bypass Couplings of Nonresonating TE/sub 10/01/ modes",

IEEE Transactions on Microwave Theory and Techniques, vol. 51, no. 6, pp. 1735-1742, June 2003, DOI: 10.1109/TMTT.2003.812577

[4] S. Bastioli, C. Tomassoni, and R. Sorrentino, "TM Dual-Mode Pseudoelliptic Filters Using Nonresonating Modes", *IEEE MTT-S Int. Microw. Symp. Dig*., Anaheim, CA, May 2010, pp. 880–883, DOI: 10.1109/MWSYM.2010.5518108

[5] S. Bastioli, L. Marcaccioli, C. Tomassoni, and R. Sorrentino, "Ultracompact Highly-Selective Dual-Mode Pseudoelliptic Filters", *IET Electronic Letter*, vol. 46, no. 2, pp. 147–149, 2010, DOI: 10.1049/el.2010.2971

[6] C. Tomassoni, S. Bastioli and R. Sorrentino, "Generalized TM Dual-Mode Cavity Filters", *IEEE Transactions on Microwave Theory and Techniques*, vol. 59, no. 12, pp. 3338-3346, Dec. 2011, DOI: 10.1109/TMTT.2011.2172622

[7] L. Pelliccia F. Cacciamani C. Tomassoni R. Sorrentino "Ultra-Compact High-Performance Filters Based on TM Dual-Mode Dielectric-Loaded Cavities", *International Journal of Microwave and Wireless Technologies,* vol. 6 no. 2 pp. 151-159, Apr. 2014, DOI: 10.1017/S1759078713001001

[8] W. Afzal, A. Ebrahimi, M. R. Robel and W. S. T. Rowe, "Low-Profile Higher-Order Narrowband Bandpass Miniaturized-Element Frequency-Selective Surface", *IEEE Transactions on Antennas and Propagation*, vol. 71, no. 4, pp. 3736-3740, April 2023, DOI: 10.1109/TAP.2023.3239171

[9] Y. Wu, K. Ma, S. Li and Y. Zhan, "Design of Vertically Integrated Folded SISL Patch Bandpass Filters with Single and Multiband Responses", *IEEE Transactions on Components, Packaging and Manufacturing Technology*, vol. 14, no. 3, pp. 479-488, March 2024, DOI: 10.1109/TCPMT.2024.3359857

[10] P. N. Choubey and W. Hong, "Dual-Band Bandpass Filter Designed by Exploiting the Second-Order Degenerated Modes of the Siw-Cavity", *2015 Asia-Pacific Microwave Conference (APMC)*, Nanjing, China, 2015, pp. 1-3, DOI: 10.1109/APMC.2015.7411657

[11] L. Yang, M. Malki and R. Gómez-García, "Multilayer Dual-Band Bandpass Filter Using Microstrip-to-Slotline Transitions and Transversal Signal-Interference Microstrip Lines", *2024 IEEE Radio and Wireless Symposium (RWS)*, San Antonio, TX, USA, 2024, pp. 79-82, DOI: 10.1109/RWS56914.2024.10438619

[12] P. Pech, S. Saron, G. Chaudhary and Y. Jeong, "Ultra-Compact Substrate Integrated Waveguide Bandpass Filter with Unequal Termination Impedance", *2023 Asia-Pacific Microwave Conference (APMC)*, Taipei, Taiwan, 2023, pp. 134-136, DOI: 10.1109/APMC57107.2023.10439966

[13] H. Liu, Y. Cheng, H. Luo, F. Chen, L. Yang and X. Li, "Reconfigurable Microstrip Bandpass Filter Based on Spoof Surface Plasmon Polaritons of M-Cusp-H-Type Cells", *IEEE Transactions on Circuits and Systems II: Express Briefs*, vol. 71, no. 6, pp. 3031-3035, DOI: 10.1109/TCSII.2024.3354768

[14] A. Zhang, J. Xu and Z. Liu, "A Microstrip Linear-Phase BPF Using Dual-Band Negative Group Delay Equalizers", *IEEE Microwave and Wireless Technology Letters*, DOI: 10.1109/LMWT.2024.3361896

[15] H. Liu, S. Wang, J. Kuang, R. Wang and H. Tian, "Compact HTS Narrowband Bandpass Filter Based on Spiral D-CRLH Resonator", *IEEE Transacions on Circuits and Systems II: Express Briefs*, vol. 71, no. 3, pp. 1007-1011, March 2024, DOI: 10.1109/TCSII.2023.3323859

[16] X. P. Lin, C. -F. Chen, R. -B. Wu and C. -S. Wang, "Realization of Miniatured Wi-Fi 6E Bandpass Filters on a Low-Loss Organic Substrate", *IEEE Transactions on Components, Packaging and Manufacturing Technology*, vol. 13, no. 11, pp. 1825-1832, Nov. 2023, DOI: 10.1109/TCPMT.2023.3319635

[17] B. Zhang et al., "Narrowband SIW-SSPP Hybrid Bandpass Filter with Compact Profile at Ka-Band", *IEEE Access*, vol. 11, pp. 98305-98314, 2023, DOI: 10.1109/ACCESS.2023.3312288

[18] X. -F. Li and J. -K. Xiao, "Dual-Band Bandpass Filter Based on Suspended Coplanar Waveguide-Microstrip Hybrid", *IEEE Transactions on Circuits and Systems I: Regular Papers*, vol. 70, no. 10, pp. 3920-3929, Oct. 2023, DOI: 10.1109/TCSI.2023.3289655

[19] M. R. A. Nasser, R. K. Jaiswal and D. Psychogiou, "A Compact Bandpass Filter Manifold with Ultrawide Frequency and Bandwidth Tuning", *IEEE Access*, vol. 11, pp. 41054-41060, 2023, DOI: 10.1109/ACCESS.2023.3269884

[20] K. L. Sheng, X. Wang, S. S. Qian, B. Sima, Z. Y. Zong and W. Wu, "Broadband Filtering Power Divider Employing Hybrid Quarter Circular/Cambered SIW Cavity and MSL Resonators", *IEEE Microwave and Wireless Technology Letters*, DOI: 10.1109/LMWT.2024.3462936

[21] N. Ji, G. Shen, W. Feng, Q. Xue and W. Che, "High Selectivity Bandpass Filter-Integrated SPDT Switch Using Switchable Dual-Mode Hybrid Resonators", *IEEE Transactions on Components, Packaging and Manufacturing Technology*, DOI: 10.1109/TCPMT.2024.3459639

[22] A. K. Nayak, V. Singh Yadav and A. Patnaik, "Wideband Transition from Tapered Microstrip to Corrugated SIW", *2019 IEEE MTT-S International Microwave and RF Conference (IMARC)*, Mumbai, India, 2019, pp. 1-4, DOI: 10.1109/IMaRC45935.2019.9118708

[23] A. K. Nayak, I. M. Filanovsky, K. Moez and A. Patnaik, "A Broadband Coaxial Line-to-SIW Transition Using Aperture-Coupling Method", *IEEE Microwave and Wireless Components Letters*, vol. 32, no. 11, pp. 1271-1274, Nov. 2022, DOI: 10.1109/LMWC.2022.3182933

[24] S. Kumari, N. K. Maurya, P. Pareek, et al. "Design and Analysis of a Novel Broadband Tweaked T-shaped Stub-loaded Quadrature Power-Splitter". *Iranian Journal of Science and Technology, Transactions of Electrical Engineering*, vol. 48, pp. 1343–1352, 2024, DOI: 10.1007/s40998-024-00711-3

[25] A. K. Nayak, I. M. Filanovsky, K. Moez and A. Patnaik, "Broadband Conductor Backed-CPW With Substrate-Integrated Coaxial Line to SIW Transition for C-Band", *IEEE Transactions on Circuits and Systems II: Express Briefs*, vol. 69, no. 5, pp. 2488-2492, May 2022, DOI: 10.1109/TCSII.2022.3160075

[26] N. K. Maurya, K. Sadhana, P. Prakash, and S. Lokendra, "Graphene-Based Frequency Agile Isolation Enhancement Mechanism for MIMO Antenna in the terahertz Regime", *Nano Communication Networks*, vol. 35, 2023, 100436, https://doi.org/10.1016/j.nancom.2023.100436

[27] A. K. Nayak, I. M. Filanovsky, K. Moez, and A. Patnaik, "A Wideband Transition from Coaxial Line to Substrate Integrated Waveguide", *IEEE Transactions on Components, Packaging and Manufacturing Technology*, vol. 14, no. 11, pp. 2011-2019, Sept. 2024, DOI: 10.1109/TCPMT.2024.3464243